

Temperature-dependent spin-wave behavior in Co/CoO bilayers studied by Brillouin light scattering

A. Ercole, W. S. Lew, G. Lauhoff,* E. T. M. Kernohan, J. Lee,[†] and J. A. C. Bland[‡]

Cavendish Laboratory, University of Cambridge, Madingley Road, Cambridge CB3 0HE, United Kingdom

(Received 5 November 1999; revised manuscript received 10 April 2000)

We report Brillouin light scattering measurements of spin-wave frequencies in exchange coupled ferromagnet (FM)/antiferromagnet (AF) epitaxial Co/CoO bilayer structures. The ultrathin (7 Å) CoO layer perturbs the Co layer spin-wave frequencies and so permits a study of the influence of the AF CoO layer at the interface, when the unidirectional anisotropy is negligible. A striking temperature dependence of the measured frequencies in the cobalt layer in the range 77 to 300 K was observed which has been demonstrated to be due to exchange coupling to the CoO layer as antiferromagnetic order develops. Furthermore, the existence of a uniaxial anisotropy field in the range 100–300 Oe within the AF layer along the FM layer magnetization direction was demonstrated. The ratio of the interface to the bulk AF exchange coupling strengths was found to lie in the range 0.75 to 1.1. The observed temperature dependence of the spin-wave linewidths indicate that locally ordered AF regions persist above the Néel temperature and play a central role in determining the magnetic behavior.

I. INTRODUCTION

Exchange biasing in strongly coupled ferromagnet/antiferromagnet (FM/AF) structures is of considerable interest due to its relevance to magnetoresistive devices.^{1,2} The effect has been attributed to the interfacial exchange interaction between the layers. There have been numerous studies^{3–7} of the exchange-biasing phenomenon since the first observation by Meiklejohn and Bean.⁸ Such studies have mainly concentrated on measurements of static properties. Various theoretical models have been proposed to describe the coupling mechanism, that include Malozemoff's random field model,⁹ Koon's spin-flop coupling model,¹⁰ Suhl's quantum mechanical approach,¹¹ and recently Schulthess's explanation to embrace both spin flop coupling and random fields.¹²

Antiferromagnetic materials are often more difficult to study than ferromagnets. The spin structure is accessible to neutron diffraction, which is sensitive to magnetic as well as structural order. Indeed, such measurements can also give the magnetization of the magnetic atoms. However, these materials have (in laboratory fields) virtually no net magnetization, which makes anisotropy measurements difficult. The spin-wave energies in antiferromagnets, which are of high energy¹³ and accessible to Raman spectroscopy, are sensitive to exchange or anisotropy fields. This has been widely applied to a number of materials, for example CoO,¹⁴ MnO, MnS,¹⁵ MnF₂,¹⁶ FeF₂.¹⁷ Such experiments have shown that the antiferromagnetic order is stabilized by the presence of truly huge anisotropies, often of complicated symmetry, which may change with temperature if the crystal structure becomes distorted.

Unfortunately, attempts to apply Raman spectroscopy to probe thin film AFs appear to have been unsuccessful, as the technique is insufficiently sensitive. Other measurement techniques include polarized neutron reflectivity (PNR) which have yielded important results, for example that per-

pendicular spin configurations can arise in FM/AF structures.¹⁸ Measurement of the spin-wave properties in the FM layer instead can provide an alternative and nondestructive method of probing the magnetic order in the AF indirectly. Using Brillouin light scattering (BLS) or ferromagnetic resonance (FMR) one can gain insight into the bulk and interface exchange coupling via the spin-wave frequencies. There have however been few measurements of spin-wave frequencies in FM/AF bilayers. In the studies reported to date,^{19–23} different analyses have been employed to gain information on the effects of the exchange bias field and magnetic anisotropy in the AF layer. Moreover, the effects of the exchange field and anisotropies on the spin-wave linewidths need to be further clarified.

In this paper, a detailed study of the temperature dependent spin-wave frequency in Co/CoO bilayers for the temperature range 77 to 300 K is presented using the BLS technique. Néel temperature T_N for cobalt oxide is around 290 K for the bulk material,²⁵ but T_N is thickness dependent in thin films as has been demonstrated (along with a scaling law)²⁴ and so can be reduced in sufficiently thin films. A marked increase in the Co spin-wave frequencies with reducing temperature in ultrathin Co/CoO bilayer structures has been previously reported.²⁶ This study prompted the development by Stamps *et al.*²⁷ of a possible theoretical description for the observed temperature-dependent behavior in terms of an exchange coupled temperature-dependent spin-configuration from the AF layer. We choose to study structures in which the CoO layer is very thin (7 Å) in order to maintain an epitaxial structure throughout the Co/CoO bilayer. For such a thin CoO layer, the T_N should be well below the lowest studied temperature of 77 K,²⁴ and the presence of such a thin layer therefore acts to perturb the Co spin-wave frequencies via the interfacial coupling. This permits a study of the influence of the AF layer spin at the interface, in the case where the interfacial coupling is too weak to give rise to a unidirectional anisotropy. The experimental results will be examined both empirically and by comparison with the predictions of a model similar to that of Ref. 27.

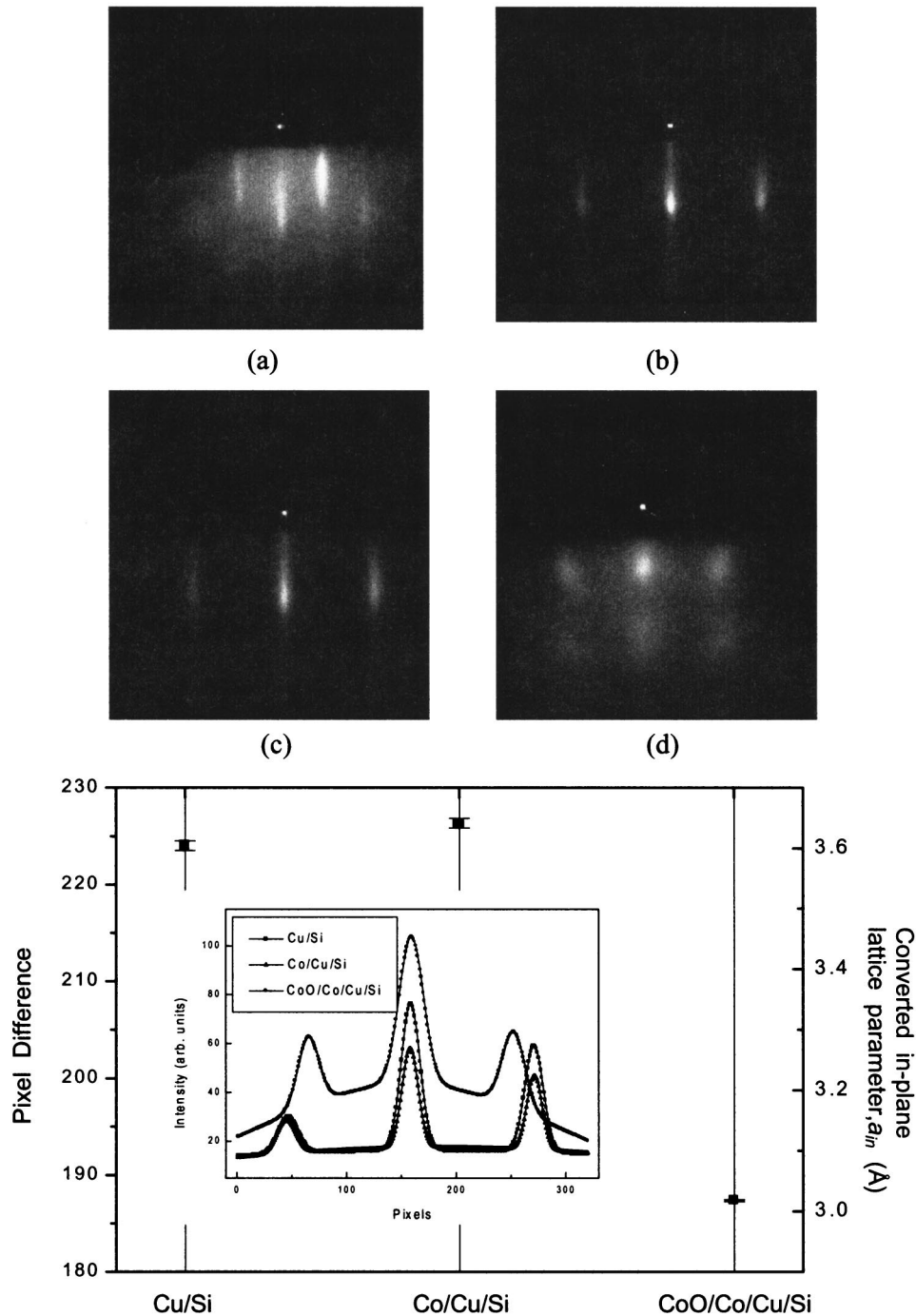


FIG. 1. Top panel: RHEED patterns at various stages of the sample growth (a) Si(001) substrate, (b) after deposition of Cu layer, (c) after Co film deposition, (d) oxidized Co surface. The angle of incidence was approximately 1° from the surface along Si[110] and the electron energy was 15 keV. Bottom panel: Pixel difference measured by RHEED and converted in-plane lattice parameter (a_{in}) for three different stages during sample growth. The a_{in} of Cu film at 1000 Å is assumed to be a_{in} of bulk Cu. The inset shows the intensity profiles that are fitted with Gaussian functions.

II. EXPERIMENTAL

A Co/CoO bilayer was grown at room temperature on a Cu/Si(001) template by molecular beam epitaxy under ultra-high vacuum conditions with a base pressure of order 10^{-10} mbar. The substrates were hydrogen passivated with aqueous HF to stabilize the surface.²⁸ After 30 Å of Co was grown, a shutter is placed to cover half of the substrate and a 30 Å Cu cap was deposited to form a control sample without an oxide layer. The sample was then oxidized for 30 min in 10^{-3} mbar of high purity oxygen, and the shutter repositioned to enable the oxidized half to be capped, again with 30 Å of Cu. Figure 1 shows the reflection high-energy electron diffraction (RHEED) images along the $\langle 110 \rangle$ azimuth of the (a) Si(001) substrate (b) 1000 Å Cu/Si(001), (c) 30 Å

Co/Cu/Si(001), and (d) the Co layer after oxidation. After completion of the Cu layer, sharp streaks with low background are observed. No qualitative change is observed in the RHEED pattern after completion of the Co layer. This agrees with the earlier finding²⁹ that three-dimensional epitaxial growth occurs along the [001] direction with the Cu and Co axis rotated in-plane by 45° with respect to the Si(001) principle axis.^{29,30} Furthermore the intensity profiles of RHEED images are measured across the streaked spots to determine the in-plane lattice parameter as shown in Fig. 1. The profiles are fitted with four Gaussian functions. The measured difference in pixel position between left and right peaks quantitatively confirms that the Co film grows coherently on the Cu film. This agrees with previous finding that

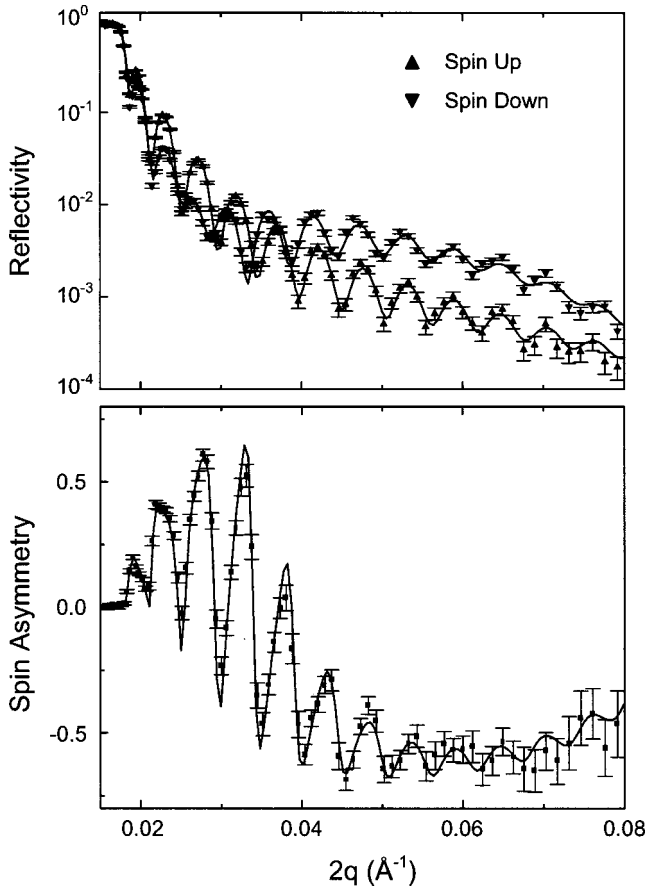


FIG. 2. PNR reflectivity and spin asymmetry data (symbol) and their best fits (continuous line) for the Cu/Co/CoO/Cu film.

Co grows coherently up to 15 ML on Cu(001).³¹ After oxidation, the RHEED pattern of the Co film becomes more spotlike. This suggests that the films are still epitaxial, although some disorder is introduced as earlier suggested.³² The in-plane parameter for the Co film becomes smaller after oxidation.

PNR experiments were carried out on the CRISP time-of-flight neutron reflectometer at the Rutherford Appleton Laboratory.^{33–34} The samples were held at 300 K with a 700 mT magnetic field applied in-plane along the direction normal to the scattering plane using an electromagnet. The beam polarization has been found to be better than 96% and the data given are corrected based on previous calibration measurements. For fitting the PNR data, the magnetic moments and layer thicknesses are adjusted. Defects, steps, interdiffusion, and local fluctuations can contribute to an effective roughness at each interface. This has the effect of reducing the specularly reflected intensity due to diffuse scattering which is taken into account by introducing a random Gaussian microscopic distribution (or vertical roughness parameter) at each interface as proposed by Nevot and Croce.³⁵ Figure 2 shows the measured and fitted spin-dependent reflectivity and spin asymmetry data for the Cu/Co/CoO/Cu film as a function of the neutron scattering vector ($2q$) perpendicular to the film plane. The spin asymmetry is given by $(R_{\text{spin-up}} - R_{\text{spin-down}})/(R_{\text{spin-up}} + R_{\text{spin-down}})$, where $R_{\text{spin-up}}$ and $R_{\text{spin-down}}$ indicate the reflectivities of the neutrons with spin parallel (spin-up) and antiparallel (spin-down) to the film magnetization, respectively. Several pronounced oscillations

TABLE I. The layer thicknesses and magnetic moments for the Cu/Co/Cu(001) and the Cu/CoO/Co/Cu(001) film as determined from PNR measurements.

	Thickness	Magnetic moment	Thickness	Magnetic moment
Cu	$56 \pm 2 \text{ \AA}$		$52 \pm 2 \text{ \AA}$	
CoO			$7 \pm 2 \text{ \AA}$	
Co	$31 \pm 2 \text{ \AA}$	$1.27 \pm 0.08 \mu_B$	$28 \pm 2 \text{ \AA}$	$1.27 \pm 0.08 \mu_B$
Cu	$928 \pm 5 \text{ \AA}$		$928 \pm 5 \text{ \AA}$	

are seen in both the reflectivity and spin asymmetry data and excellent fits to the data are obtained throughout the entire q range studied. Similar quality fits are obtained to the Cu/Co/Cu sample. The magnetic moments, layer thicknesses and interface roughness obtained from the fits are shown in Table I for both the Cu/Co/Cu and Cu/Co/CoO/Cu samples. For the Co film a magnetic moment of $1.27 \pm 0.08 \mu_B$ /atom is determined, which is slightly lower than the bulk moment of $1.74 \mu_B$ /atom for fcc Co or $1.71 \mu_B$ /atom for hcp Co at room temperature.³⁶ This is presumably due to the presence of residual carbon and oxygen impurities in the Co film as observed in the Auger electron spectroscopy (AES). Also a mean vertical interfacial roughness of about 12 \AA is obtained from the PNR measurements. The fit to the PNR data for the oxidized Co film yields a Co layer thickness of 28 \AA and a CoO layer thickness of approximately 7 \AA .

Ex situ magneto-optical Kerr effect (MOKE) measurements (Fig. 3) show the samples to have fourfold in-plane anisotropy. The oxidized sample show an increased coercivity over the control Co sample as is to be expected from the increased surface disorder shown by the RHEED measurements. Our BLS system uses a Sandercock 3+3 pass tandem Fabry-Perot interferometer³⁷ with a computer-based stabilization system,³⁸ which gives high immunity to vibration. For the low temperature measurements, the sample was mounted in a customized gas flow cryostat.

III. RESULTS AND DISCUSSION

A representative BLS spectrum taken with the sample held at room temperature is shown in Fig. 4. For this thickness, only surface-type^{39–40} modes are observed. The broad lines, which have been seen before in Co films⁴¹ are considerably wider than the instrument response function. The line width in the oxide sample is seen to be larger still, presumably due to increased surface disorder or structural inhomogeneities.

Measurements of the spin-wave frequency as a function of in-plane applied field angle and strength allow the magnetic parameters of the samples to be deduced.⁴² Angular dependent results in Fig. 5 show that the predominant anisotropy is of fourfold symmetry, as is to be expected for fcc Co. The data from the control Co sample could be well modeled by assuming an anisotropy field $K_1/M = -500 \text{ Oe}$ (making the Co[100] direction hard), $g = 2.30$. It is necessary to include a small uniaxial anisotropy field, $K_u/M = 35 \text{ Oe}$. From these results, we can deduce the value of the surface anisotropy K_s (for a definition see, for example, Ref. 43) which is found to be -0.5 erg cm^{-1} (i.e., favoring in-plane magneti-

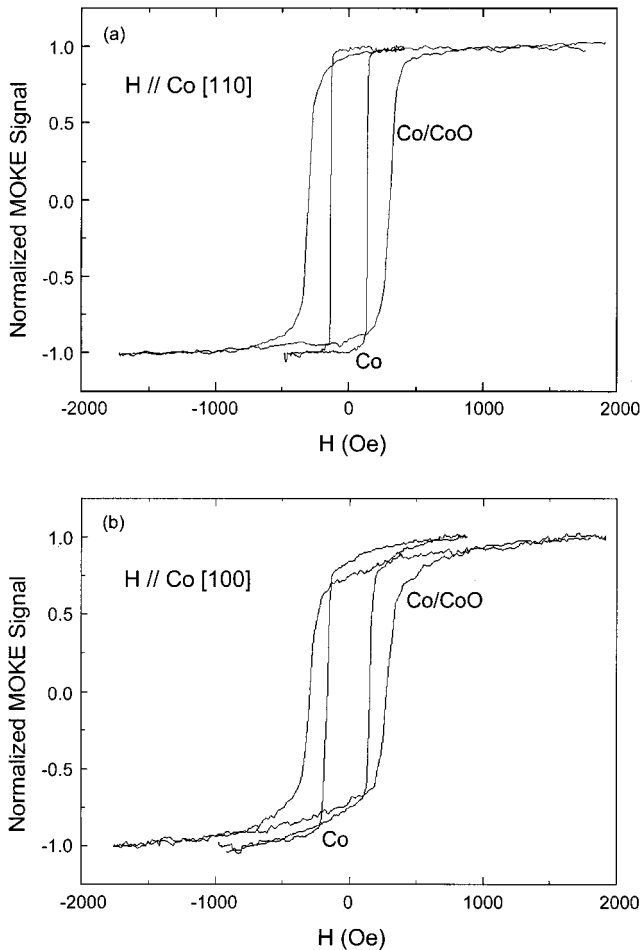


FIG. 3. Room temperature in-plane MOKE measurements showing increased (a) easy- and (b) hard-axis coercivity in the Co/CoO sample.

zation). The angle scan from the Co/CoO sample could be fitted using the layer thicknesses and Co layer magnetization from the PNR measurements. It is not necessary to adjust the in-plane anisotropies. K_s is found to be reduced to -0.3 erg cm^{-1} due to the difference between the Co/CoO and Co/Cu interfaces. If it is assumed that the two Co/Cu interfaces in the control sample are equivalent then one can infer a value of $K_s = -0.1 \text{ erg cm}^{-1}$ for the Co/CoO interface.

Spin-wave linewidths are also measured as functions of azimuth and the data is presented in Fig. 5 for an applied field of 8.5 kOe. The BLS linewidth (FWHM) is determined from the spectra by fitting peaks with Gaussian functions. The angular dependence of the line width in both samples shows a fourfold variation. However, for the control Co sample, this behavior follows the frequency whereas the oxidized sample shows the reverse behavior. The average spin-wave line width shows an increase ($\sim 5 \text{ GHz}$) in the oxidized sample compared to that of the control Co sample, as is characteristic of a spin disorder effect. At high fields, the line widths are found to be substantially independent of field magnitude. This implies that the spin-wave damping is substantially due to an extrinsic mechanism.⁴⁴

Figure 6 shows the temperature dependence of the spin-wave frequency as the sample is cooled in steps of 25 K with magnetic field applied along either the easy or hard crystal-

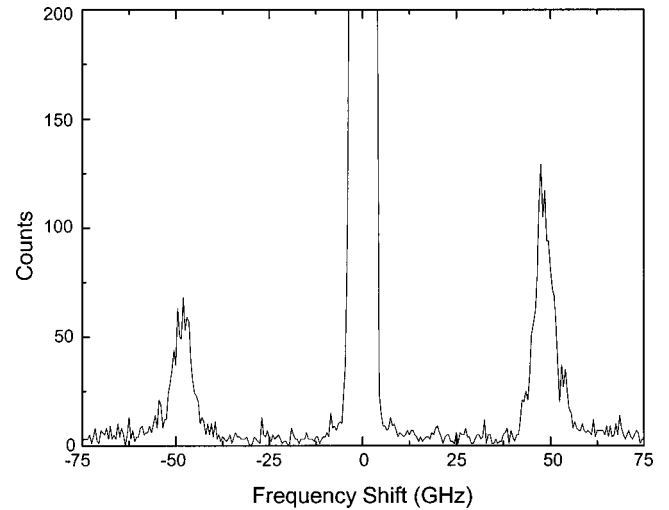


FIG. 4. Representative BLS spectrum taken at room temperature. The applied field was 8.5 kOe and was oriented along the Co[100] direction. The large feature in the center is due to elastic scattering from the sample. Surface-type modes are seen in both the high frequency (anti-Stokes) and low frequency (Stokes) sides of the spectra.

lographic axes. As BLS probes thermally excited spin waves it follows that, at low temperatures, the intensity of the scattered signal is reduced. Typical acquisition times are around 15 h per spectrum. The frequency can be seen to increase as the temperature is reduced as expected. Similar measurements for the control Co sample show no detectable variation

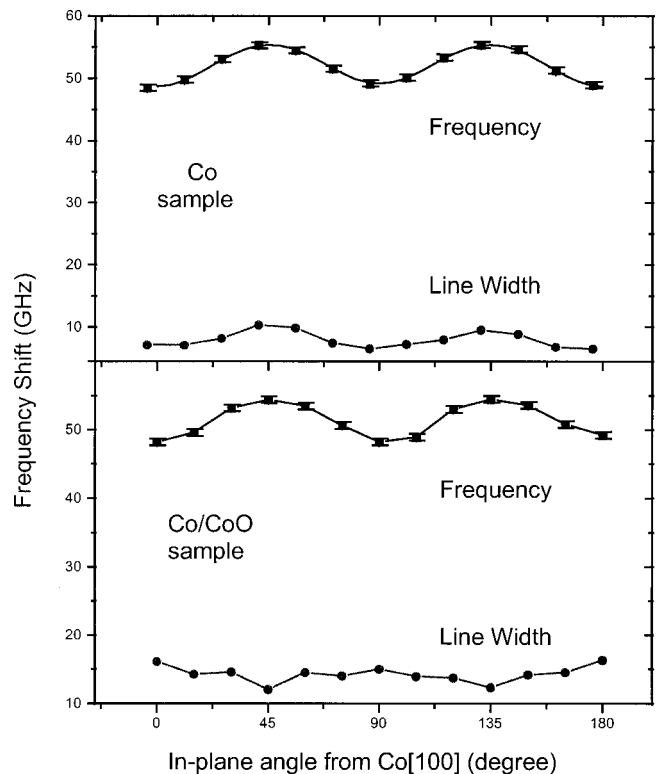


FIG. 5. Spin-wave frequencies and line widths plotted against in-plane field angle for the Co sample and the Co/CoO sample at room temperature. The applied field was 8.5 kOe and the angle of incidence was 45° .

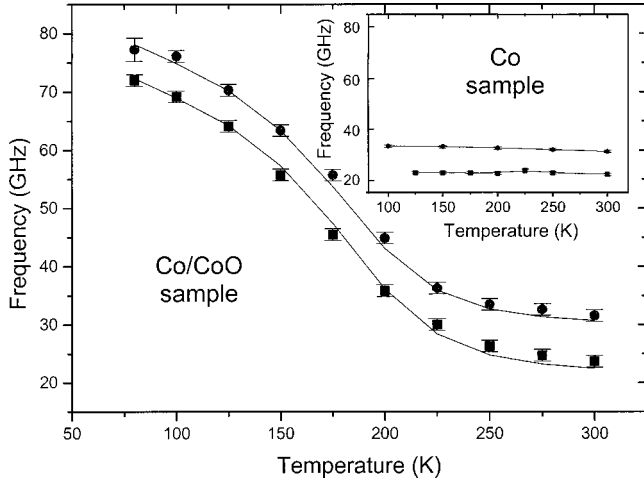


FIG. 6. Temperature dependence of Co spin-wave frequency for fields directed along easy (Co[110]-top curve) and hard (Co[100]-lower curve) axes. The lines are fitted by a mean field model as described in the text. By contrast, the unoxidized sample (inset) shows no detectable change in frequency with temperature.

in frequency, indicating that the cubic anisotropy is temperature independent within errors, also justifying the assumption of a constant Co moment. Low-temperature angle-dependent scans confirm that no unidirectional anisotropy occurs as expected.

The variation of the spin-wave peak intensity with temperature is shown in the upper panel of Fig. 7 for the hard axis. Similar data is obtained for the easy axis. Such intensity measurements can be sensitive to statistical noise, and so a large number of measurements have been made at low temperatures where the counting statistics are poor. These give confidence that the fifteen-hour acquisition times used are sufficient. The intensity of both the Stokes and anti-Stokes lines can be seen to decrease with falling temperature.

The lower panel of Fig. 7 shows the mode line width as a function of temperature. The instrument broadening is approximately 0.5 GHz. It is clear that a significant broadening occurs as the temperature is reduced. As the temperature is lowered and the AF layer begins to order magnetically, the spin waves in the FM layer begin to experience the effect of spin disorder both due to structural inhomogeneities and thermal fluctuations in the AF layer by virtue of the interface coupling. Linewidth studies for the unoxidized sample showed no such behavior and accordingly, the intensity variations are found to be much smaller.

A. Mean field model

A mean field theory has been described by Stamps and co-workers.²⁷ Some extensions to this model are necessary when working with a system with an additional strong in-plane anisotropy. The spin-wave excitations in magnetic materials correspond to thermally excited spin precessions, and are described by solutions to the Landau-Lifshitz (LL) torque equation

$$\frac{\partial \mathbf{M}}{\partial t} = \gamma(\mathbf{M} \times \mathbf{H}_i), \quad (1)$$

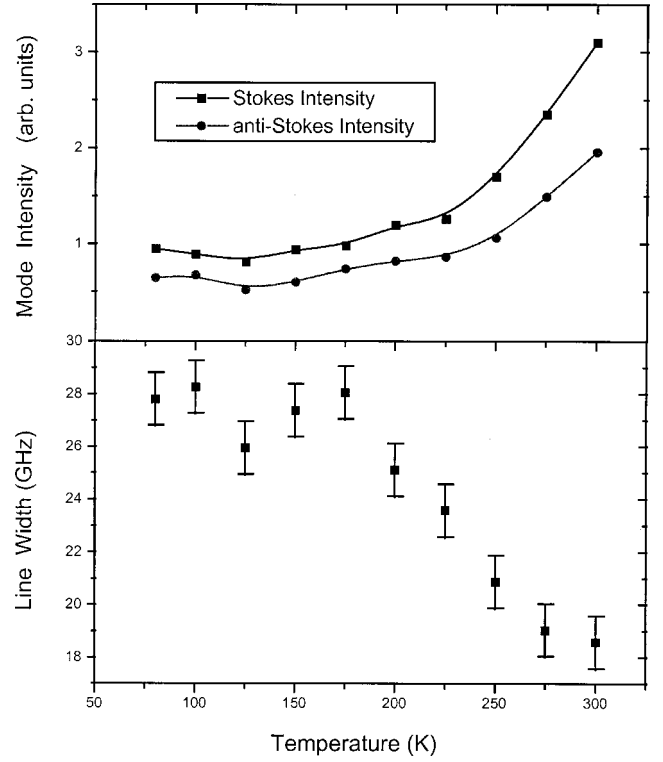


FIG. 7. Top panel: spin-wave peak intensity of the Co/CoO sample measured along the hard axis plotted against temperature for the Stokes and anti-Stokes modes. Bottom panel: spin-wave line width of the Co/CoO sample plotted against temperature.

where \mathbf{M} is the magnetization, γ is the gyromagnetic ratio (proportional to the g factor) and \mathbf{H}_i is the sum of all fields present in the sample which may be external in origin, or may be internal due to exchange or magnetocrystalline anisotropy.

The structure is modeled as a number of atomic layers (see Fig. 1 of Ref. 27) and the magnetic atoms in the CoO are assumed to be layer-by-layer antiparallel, so that only vertical coupling between layers needs to be considered. Horizontally adjacent spins are always parallel and incur no exchange energy penalty: this means only spin waves with zero wave vectors will be considered. The y axis is normal to the films' surfaces, and we assume an external field H_0 is applied in-plane along the z axis. Also, only nearest neighbor exchange interactions are taken into account.

We may write the effective field \mathbf{H}_i on spins \mathbf{S}_i in the i th layer as is the sum of the external fields, the dipolar fields, the anisotropy fields, as well as the exchange field from the spins in the layers above and below as

$$\begin{aligned} \mathbf{H}_i = & \frac{1}{g\mu_B} [J_{i,i-1}\mathbf{S}_{i-1} + J_{i,i+1}\mathbf{S}_{i+1}] + H_i^{\text{in}}(S_i^z/S)\mathbf{i}_z \\ & + (H_i^{\text{out}} - 4\pi M)(S_i^y/S)\mathbf{i}_y + H_i^x\mathbf{i}_x + H_i^y\mathbf{i}_y + H_0^z\mathbf{i}_z. \quad (2) \end{aligned}$$

The symbols g , H^{in} , and H^{out} represent the g factor, the in-plane uniaxial anisotropy field, and the out-of-plane uniaxial anisotropy field, respectively. The parameter $J_{m,n}$ represents the exchange coupling constant between the m th

and n th layers. This takes one of three values representing the FM(J_{FM}), AF(J_{AF}), or interface (J_{int}) exchange coupling strengths.

For fcc Co, we also need to introduce a fourfold cubic anisotropy of magnitude K_1 . The anisotropy field can be expressed as

$$\mathbf{H}^{\text{ani}} = -\frac{1}{M} \nabla_u F_{\text{ani}}, \quad (3)$$

where F_{ani} is the cubic anisotropy energy and the gradient operator is taken with respect to the components of the magnetization unit vector. \mathbf{H}^{ani} is solved for the i th layer into in- and out-of-plane components which are, respectively,

$$H_i^x = \frac{2K_{1,i}}{M} (1 - 8 \sin^2 \phi_i + 8 \sin^4 \phi_i), \quad (4)$$

$$H_i^y = \frac{2K_{1,j}}{M} (1 - 2 \sin^2 \phi_i + 2 \sin^4 \phi_i). \quad (5)$$

All the constants are assumed to be temperature independent: the temperature dependence is introduced²⁷ by replacing the spin magnitudes by their (reduced) thermal averages using a Brillouin function approach. The temperature of the FM layers was set to absolute zero. This is equivalent to assuming that J_{FM} is large enough that the magnetic state of the Co layer does not change appreciably over the temperature range investigated.

To solve for the spin-wave mode frequencies, a harmonic time dependence is assumed for each \mathbf{S}_i and the relationships above are substituted into the LL equation $d\mathbf{S}_i/dt = \gamma(\mathbf{S}_i \times \mathbf{H}_i)$, which can then be expressed in matrix form once terms quadratic in S_x and S_y have been neglected. This is equivalent to the assumption that the spin precession amplitudes are small. The resulting matrix equation can be solved to find its eigenvalues, which give the frequencies of the various possible spin-wave modes.

The curves in Fig. 6 are the result of a fit to the model described above. In fitting the data, all magnetic parameters for the Co layer are fixed according to the room temperature BLS angle and field scans results as discussed above. The exact value of the J_{FM} is not relevant: it is large enough that the magnetic state of this layer does not change appreciably over the temperature range investigated.

Within the model, only the CoO magnetic parameters have been varied to modify the predicted magnitude and onset of the temperature dependence. The critical temperature is governed almost entirely by the value of the J_{AF} (found to be -365 ± 5 Oe). It is not necessary to include H^{out} or a fourfold anisotropy in the CoO layer in order to obtain a fit to the data. The assumption that H^{out} to be 0 for the CoO is reasonable since the layer is quite rough (evidence from the RHEED pattern), so out-of-plane anisotropy is likely to be small at this thickness. The mode frequencies are also insensitive to the parameter of magnetization M_{CoO} .

The magnitude of the temperature rise is governed by both the H^{in} and the J_{int} : it is not possible to determine these parameters independently. However, if the J_{int} is assumed to be equal to that in the bulk AF layer (i.e., $J_{\text{int}} = J_{\text{AF}}$) then a value of $H^{\text{in}} = 120 \pm 10$ Oe is deduced for the in-plane anisotropy

of the AF layer. Despite the degeneracy in these parameters, by varying the J_{int} and refitting it is possible to determine that $100 \text{ Oe} < H^{\text{in}} < 300 \text{ Oe}$ for the CoO and that $0.75J_{\text{AF}} < J_{\text{int}} < 1.1J_{\text{AF}}$.

There have been various antiferromagnetic resonance studies of CoO.^{14,15} These studies have determined the anisotropies acting in bulk samples of CoO. Note that the value of H^{in} deduced in this experiment is two orders of magnitude smaller than any literature value. Furthermore the crystal field and anisotropies in bulk specimens are known to give rise to a CoO easy axis along the $[11\bar{7}]$ direction.¹⁵ By contrast, the model of Ref. 27 here achieves a good fit by assuming that the AF easy axis is parallel to the FM magnetization.

B. Critical exponent model

In order to determine the critical temperature for the onset of the AF order we may fit both temperature dependencies separately using a critical exponent model. Within the Landau theory of phase transitions, it is common to assign an order parameter Ψ to the system of interest. It is defined so as to vary monotonically as the system changes state between one phase and the other having the value zero when the system is in one phase, and unity (by convention) when the phase change is complete. The energy of the system can then conveniently be expressed as a power series in Ψ . If the phase transition proceeds as a function of a temperature, then the order parameter can be described by an expression of the form

$$\begin{aligned} \Psi_f(T) &= \left(1 - \frac{T}{T_c}\right)^\eta \\ &= f(T) - f(\infty) \\ &\approx f(T) - f(300 \text{ K}) \text{ for } T < T_c, \end{aligned} \quad (6)$$

where T_c is a critical temperature for the transition, and the parameter η is known as the critical exponent. The term $f(T)$ refers to either the frequency $\omega(T)$ or the linewidth $\Delta\omega(T)$. The approximate of the above expression is justified on the basis that both $\omega(T)$ and $\Delta\omega(T)$ are approximately temperature independent by 300 K. From Eq. (6), it is seen that the gradient of the order parameter increases monotonically with rising temperature until T_c is reached, at which point the model no longer holds.

The best fits are shown in Fig. 8. The fitted values for the parameter set $\{T_c, \eta\}$ were found to be $\{207 \text{ K}, 0.5\}$ and $\{250 \text{ K}, 0.4\}$ for the frequency and linewidth data respectively. The spin wave frequency increases monotonically from its high temperature value as the temperature is reduced. If the observed low temperature increase in frequency is indeed due to the ordering of the AF to which the FM is coupled, then it follows that, as the system become completely ordered, the FM mode frequency must either saturate, or diverge. Such a divergence would suggest an infinite restoring torque, and it is difficult to see where such forces could originate in a closed system. We therefore conclude that the spin wave frequency will be at a maximum when the system is completely ordered.

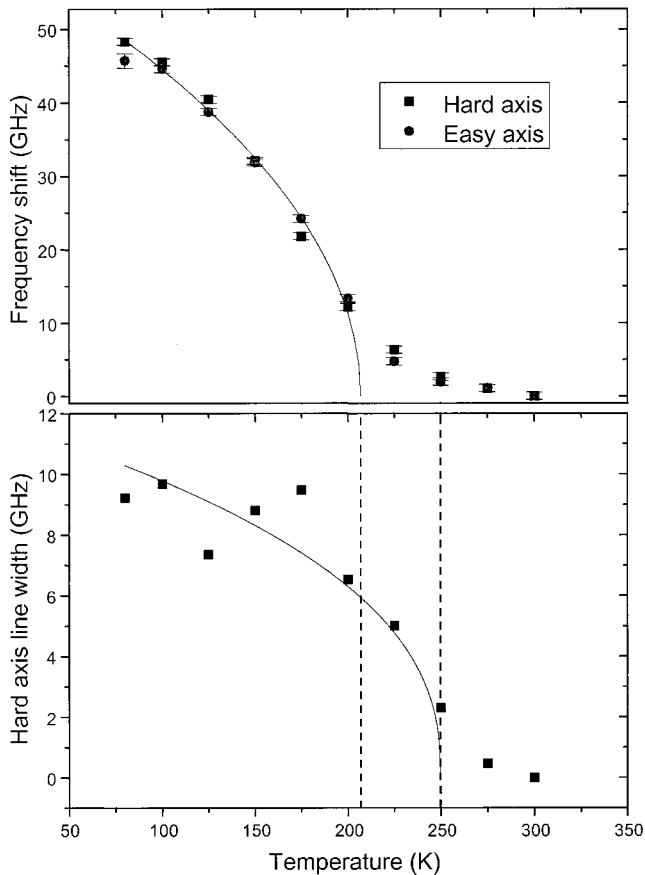


FIG. 8. Best fits of critical exponent model for the frequency and linewidth data as functions of temperature.

It is interesting to note that the critical temperatures for these processes are different, indicating that the increase in frequency and the line width broadening with reducing temperature are due to different ordering processes. We may speculate on the microscopic origin of these effects. That the value of T_c for the former process is lower than that for the latter suggests that $\omega(T)$ is governed by the magnetic ordering within the “bulk” of the AF layer, whereas $\Delta\omega(T)$ is controlled by small ill-connected regions of the AF (probably at the interface) which are able to maintain their magnetic order up to higher temperatures. Such regions correspond to locally AF ordered spins, but the random relative arrangement of these regions gives rise to the increase in line width. The individual contributions to the exchange strength reflect statistical variations in surface roughness, oxide composition and/or bulk structural imperfections. The total exchange strength will increase to a limiting value at low temperature. The spin-wave line width, however, is sensitive not to the total exchange strength, but to the fluctuations in the exchange and is affected only by disordered regions of the AF layer.

IV. CONCLUSION

Epitaxial Co/CoO bilayer structures on Si(001)/Cu substrates have been prepared. A room temperature characterization has been carried out using BLS and PNR, and a value of -0.1 erg cm^{-1} has been found for the surface anisotropy constant for the Co/CoO interface. Low temperature BLS results show a temperature dependence of the Damon-Eshbach spin-wave mode in these epitaxial fcc Co/CoO bilayers. These experiments have shown that the observed increase in frequency with reducing temperature is well described by a model similar to that of Ref. 27. The observed increase in mode frequency with decreasing temperature is attributed to the onset of AF order in the CoO layer. This result demonstrates that interface exchange coupling occurs in the absence of the unidirectional anisotropy. Angle-dependent measurements were performed but did not reveal any unidirectional anisotropy as expected for such a thin CoO layer. Such a variation, if it exists, is likely to be within the errors of the experiment.

A study of the mode line width shows a broadening with reducing temperature. This is attributable to additional random fields in the Co layer due to the CoO. Evidence for the existence of an ensemble of ordering processes present in these samples has been presented. More fundamentally, from the room temperature data, it would appear that the damping mechanisms are different for the Co/CoO bilayer as compared to the control Co sample. The angular dependence of the line width in both samples shows a fourfold variation. However, for the control Co sample, this behavior follows the frequency whereas the oxidized sample seems to show the reverse behavior. The spin-wave linewidth shows a slight increase in the oxidized sample compared to that of the control Co sample, as is also characteristic of a spin disorder effect. We conclude from the clear difference in the line width behavior of the two samples that spin disorder exists in the AF/CoO layer at the interface. Moreover, the linewidth increases as the temperature is reduced. These results demonstrate that even in the absence of an exchange bias field (giving rise to a unidirectional anisotropy) associated with the fully AF order state, line width broadening can occur due to the presence of the AF layer.²² Furthermore, we have shown that there is a well-defined uniaxial anisotropy in the AF layer above the Néel temperature.

ACKNOWLEDGMENTS

We acknowledge the support of EPSRC (U.K.) and the Cambridge Commonwealth Trust. We are grateful to Dr. S. Langridge and Dr. J. Penfold for their help with the PNR measurements.

*Present address: Toyota Technological Institute, 2-12-1 Hisakata Tempaku, 468-8511 Nagoya, Japan.

[†]Present address: Department of Physics, Atomic Scale Surface Science Research Center, Yonsei University, Seoul 120-74 Korea.

[‡]Electronic address: jacbl@phy.cam.ac.uk

¹B. Dieny, V. S. Speriosu, S. S. P. Parkin, B. A. Gurney, D. R.

Wilhoit, and D. Mauri, Phys. Rev. B **43**, 1297 (1991).

²S. S. P. Parkin, K. P. Roche, M. G. Samant, P. M. Rice, R. B. Beyers, R. E. Scheuerlein, E. J. O'Sullivan, S. L. Brown, J. Bucchigano, D. W. Abraham, Yu Lu, M. Rooks, P. L. Trouiloud, R. A. Wanner, and W. J. Gallagher, J. Appl. Phys. **85**, 5828 (1999).

- ³T. J. Moran, J. M. Gallego, and I. K. Schuller, *J. Appl. Phys.* **78**, 1887 (1995).
- ⁴R. P. Michel, A. Chaiken, C. T. Wang, and L. E. Johnson, *Phys. Rev. B* **58**, 8566 (1998).
- ⁵De-Hua Han, Jian-Gang Zhu, and J. H. Judy, *J. Appl. Phys.* **81**, 4996 (1997).
- ⁶T. Ambrose, R. L. Sommer, and C. L. Chien, *Phys. Rev. B* **56**, 83 (1997).
- ⁷V. Ström, B. J. Jönsson, K. V. Rao, and D. Dahlberg, *J. Appl. Phys.* **81**, 5003 (1997).
- ⁸W. H. Meiklejohn and C. P. Bean, *Phys. Rev.* **102**, 1413 (1956); **105**, 904 (1957).
- ⁹A. P. Malozemoff, *J. Appl. Phys.* **63**, 3874 (1988); *Phys. Rev. B* **35**, 3679 (1987).
- ¹⁰N. C. Koon, *Phys. Rev. Lett.* **78**, 4865 (1997).
- ¹¹H. Suhl and I. K. Schuller, *Phys. Rev. B* **58**, 258 (1998).
- ¹²T. C. Schulthess and W. H. Butler, *Phys. Rev. Lett.* **81**, 4516 (1998); *J. Appl. Phys.* **85**, 5510 (1999).
- ¹³M. G. Cottam and D. R. Tilley, *Introduction to Surface and Superlattice Excitations* (Cambridge University Press, Cambridge, 1989).
- ¹⁴R. R. Hayes and C. H. Perry, *Solid State Commun.* **14**, 173 (1974).
- ¹⁵H-h. Chou and H. Y. Fan, *Phys. Rev. B* **13**, 3924 (1976).
- ¹⁶F. M. Johnson and A. H. Nethercot, *Phys. Rev.* **114**, 705 (1959).
- ¹⁷M. T. Hutchings, B. D. Rainford, and H. J. Guggenheim, *J. Phys. C* **3**, 307 (1970).
- ¹⁸Y. Ijiri, J. A. Borchers, R. W. Erwin, S. H. Lee, P. J. van der Zaag, and R. M. Wolf, *Phys. Rev. Lett.* **80**, 608 (1998); J. A. Borchers, Y. Ijiri, D. M. Lind, P. G. Ivanov, R. W. Erwin, S. H. Lee, and C. F. Majkrzak, *J. Appl. Phys.* **85**, 5883 (1999).
- ¹⁹R. E. Camley and R. J. Aсталos, *J. Magn. Magn. Mater.* **198–199**, 402 (1999).
- ²⁰J. C. Scott, *J. Appl. Phys.* **57**, 3681 (1985).
- ²¹C. Mathieu, M. Bauer, B. Hillebrands, J. Fassbender, G. Güntherodt, R. Jungblut, J. Kohlhepp, and A. Reinders, *J. Appl. Phys.* **83**, 2863 (1998).
- ²²P. Miltényi, M. Gruyters, G. Güntherodt, J. Nogués, and I. K. Schuller, *Phys. Rev. B* **59**, 3333 (1999).
- ²³R. D. McMichael, M. D. Stiles, P. J. Chen, and W. F. Egelhoff, Jr., *Phys. Rev. B* **58**, 8605 (1998).
- ²⁴T. Ambrose and C. L. Chien, *Phys. Rev. Lett.* **76**, 1743 (1996).
- ²⁵*Handbook of Physical Quantities*, edited by I. S. Grigoriev and E. Z. Meilikhov (CRC Press, Boca Raton, 1997).
- ²⁶A. Ercole, T. Fujimoto, M. Patel, C. Daboo, R. J. Hicken, and J. A. C. Bland, *J. Magn. Magn. Mater.* **156**, 121 (1996).
- ²⁷R. L. Stamps, R. E. Camley, and R. J. Hicken, *Phys. Rev. B* **54**, 4159 (1996); *J. Appl. Phys.* **81**, 4485 (1997).
- ²⁸J. Lee, G. Lauhoff, M. Tselepi, S. Hope, P. Rosenbusch, J. A. C. Bland, H. A. Dürr, G. van der Laan, J. Ph. Schillé, and J. A. D. Matthew, *Phys. Rev. B* **55**, 15 103 (1997).
- ²⁹R. Naik, A. Poli, D. McKague, A. Lukaszew, and L. E. Wenger, *Phys. Rev. B* **48**, 1008 (1993).
- ³⁰B. G. Demczyk, V. M. Naik, A. Lukaszew, R. Naik, and G. W. Auner, *J. Appl. Phys.* **80**, 5035 (1996).
- ³¹O. Heckmann, H. Magnan, P. le Fevre, D. Chandesris, and J. J. Rehr, *Surf. Sci.* **312**, 62 (1994).
- ³²L. Smardz, U. Koebler, and W. Zinn, *J. Appl. Phys.* **71**, 5199 (1992).
- ³³*Ultrathin Magnetic Structures I*, edited by J. A. C. Bland and B. Heinrich (Springer-Verlag, Berlin, 1994).
- ³⁴J. Penfold, *Physica B* **173**, 1 (1991).
- ³⁵L. Nevot and P. Croce, *Rev. Phys. Appl.* **15**, 761 (1980).
- ³⁶S. Chikazumi, *Physics of Ferromagnetism* (Clarendon Press, Oxford, 1997).
- ³⁷R. Mock, B. Hillebrands, and J. R. Sandercock, *J. Phys. E* **20**, 656 (1987).
- ³⁸B. Hillebrands, *Rev. Sci. Instrum.* **70**, 1589 (1999).
- ³⁹C. E. Patton, *Phys. Rep.*, *Phys. Lett.* **103**, 251 (1984).
- ⁴⁰R. W. Damon and J. R. Eshbach, *J. Phys. Chem. Solids* **19**, 308 (1961).
- ⁴¹P. Krams, F. Lauks, R. L. Stamps, B. Hillebrands, and G. Güntherodt, *Phys. Rev. Lett.* **69**, 3674 (1992).
- ⁴²R. J. Hicken, D. E. P. Eley, M. Gester, C. Daboo, A. J. R. Ives, and J. A. C. Bland, *J. Magn. Magn. Mater.* **145**, 278 (1995).
- ⁴³B. Heinrich and J. F. Cochran, *Adv. Phys.* **42**, 523 (1993).
- ⁴⁴V. Kambersky, *Czech. J. Phys., Sect. B* **26**, 1366 (1976).